

## Locally sparse varying coefficient mixed model with application to longitudinal microbiome differential abundance

Simon Fontaine<sup>1,6,\*</sup>, Nisha J. D'Silva<sup>2,3</sup>, Marcell Costa de Medeiros<sup>2</sup>

Grace Y. Chen<sup>4</sup>, Ji Zhu<sup>1</sup>, and Gen Li<sup>5</sup>

<sup>1</sup>Department of Statistics, University of Michigan, Ann Arbor, MI, United States

<sup>2</sup>Department of Periodontics and Oral Medicine, University of Michigan, Ann Arbor, MI, United States

<sup>3</sup>Department of Pathology, University of Michigan, Ann Arbor, MI, United States

<sup>4</sup>Department of Internal Medicine, University of Michigan, Ann Arbor, MI, United States

<sup>5</sup>Department of Biostatistics, University of Michigan, Ann Arbor, MI, United States

<sup>6</sup>Department of Statistics, Pennsylvania State University, University Park, PA, United States

\*email: simfont@umich.edu

**SUMMARY:** Differential abundance (DA) analysis in microbiome studies has recently been used to uncover a plethora of associations between microbial composition and various health conditions. While current approaches to DA typically apply only to cross-sectional data, many studies feature a longitudinal design to better understand the underlying microbial dynamics. To study DA in longitudinal microbial studies, we introduce a novel varying coefficient mixed-effects model with local sparsity. The proposed method can identify time intervals of significant group differences while accounting for temporal dependence. Specifically, we exploit a penalized kernel smoothing approach for parameter estimation and include a random effect to account for serial correlation. In particular, our method operates effectively regardless of whether sampling times are shared across subjects, accommodating irregular sampling and missing observations. Simulation studies demonstrate the necessity of modeling dependence for precise estimation and support recovery. The application of our method to a longitudinal study of mice oral microbiome during cancer development revealed significant scientific insights that were otherwise not discernible through cross-sectional analyses. An R implementation is available at [github.com/fontaine618/LSVCMM](https://github.com/fontaine618/LSVCMM).

**KEY WORDS:** local regression; functional data analysis; semiparametric regression; kernel smoothing; function-on-scalar regression.

## 1. Introduction

The modern science and healthcare sectors have seen profound advancements with the emergence of omics data, such as (meta-)genomics, transcriptomics, and proteomics, among others. In particular, many studies collect omics longitudinally, which can provide researchers with greater insight into the dynamical complexities underlying a myriad of biological processes. A natural statistical question that emerges from temporal omics is that of longitudinal differential analysis (LDA), where the goal is to identify biomarkers with differences between conditions over time. Our motivating application involves the field of *microbiomics*, where differential analysis usually takes the name of *differential abundance analysis* (DAA), referring to the *abundance* of various organisms in a system of interest. Specifically, we are interested in the microbial composition in some tissue and its temporal association with multiple conditions simultaneously. The microbiota is known to play a key role in a wide range of diseases and health conditions ([Gomaa, 2020](#); [Ogunrinola et al., 2020](#)), and identifying taxa that differ in their abundance between conditions can lead to better diagnosis, prevention, and treatment.

We begin by describing the desirable properties of an LDA method. First, the estimated differences need to be smooth over time, as there is generally no expectation of discontinuous jumps. Additionally, smoothing may increase the power of the method as it allows us to borrow strength across neighboring time points. Second, the longitudinal nature of the data implies serial correlation within subjects, and failure to account for it may hinder the statistical properties of the method. Third, accomodating irregular designs demands a methodology that does not require all subjects to be measured at a common set of time points. Indeed, many studies have missing data, or samples may be collected irregularly in observational studies. Fourth, the methodology must be able not only to identify if there is a difference between conditions (*global* differences), but it must also determine the time

interval(s) where the difference occurs (*local* differences). Fifth, the methodology must allow for more complicated regression designs than simple group comparisons: for example, our motivating application involves interactions and covariate adjustments.

*Varying coefficient models* (VCMs) are natural candidates for LDA because their flexible semiparametric linear model structure can be customized for many purposes. Still, we found no existing methodology that satisfies all the above requirements. Many early work for regularized VCMs only allows global sparsity with the goal of selecting variables, not time points (Wang et al., 2008; Wang and Xia, 2009; Noh and Park, 2010; Lee and Mammen, 2016; Xue and Qu, 2012; Daye et al., 2012). The idea of local sparsity was first introduced by Wang and Kai (2015) and Kong et al. (2015) using B-splines and kernel smoothing, respectively. When using B-splines, local sparsity can be achieved by penalizing groups of consecutive spline weights, and some type of overlapping group penalty must be used. In Wang and Kai (2015), a group bridge penalty is used to induce local sparsity in a single varying intercept; Tu et al. (2020) extended the approach to more general VCMs. Zhong et al. (2022) consider instead an application of the functional SCAD penalty of Lin et al. (2017) and extend the methodology beyond least squares and to asynchronous covariates. When using kernel smoothing, local sparsity is simpler to achieve, as the evaluation of the varying coefficients can be directly penalized. In Kong et al. (2015), which considers a local linear approximation, a SCAD penalty is applied to a combination of the degree 0 and degree 1 parameters of the local linear model. However, none of the aforementioned methods adjusts for temporal dependency in their estimation procedure. Wang et al. (2022) consider a B-spline approach with a group bridge penalty on the spline weights and adjust for within-subject dependency using a two-step estimator. However, estimation of serial correlation requires all subjects to be sampled at a common set of time points, which can be prohibitive.

There exist a few methods performing longitudinal differential abundance analysis through testing rather than through sparsity-inducing penalties. A first set of methods builds on the concept of *smoothing spline analysis of variance* (SS-ANOVA, [Gu, 2013](#)) by proposing area ratio test statistics to find intervals of group differences between conditions ([Paulson et al., 2017](#); [Luo et al., 2017](#); [Metwally et al., 2018, 2022](#)). Alternatively, [Shields-Cutler et al. \(2018\)](#) propose a LOESS approach, where permutations are used to identify differential intervals. Again, the previous methods do not account for the dependency within the subject. [Staicu et al. \(2015\)](#) propose a global test for equality of means between groups, accounting for longitudinal effects and based on Fourier expansions. Unfortunately, all these testing procedures are limited to group comparisons.

We therefore propose a novel approach for local sparsity in VCMs, accounting for within-subject dependency, called LSVCMM (for *locally sparse varying coefficient mixed model*). Specifically, we consider locally-constant kernel smoothing for a VCM with parametric working covariance and obtain local and global sparsity through an adaptive sparse group Lasso ([Friedman et al., 2010](#); [Simon et al., 2013](#)). An extended Bayesian information criterion is proposed to perform tuning parameter selection, and simultaneous confidence bands are obtained through a bootstrap procedure. An R implementation is provided in the `LSMCMM` package available at [github.com/fontaine618/LSVCMM](https://github.com/fontaine618/LSVCMM). In Section 3, we conduct extensive simulation studies showing that LSVCMM improves estimation accuracy and support recovery compared to methods lacking longitudinal dependence adjustment or smoothness, or methods requiring imputation in irregular designs. In Section 4, we apply LSVCMM to a longitudinal differential analysis task that involves microbiome samples from mice with varying sex, genotype and disease status.

## 2. Methods

### 2.1 Setting & Notation

We consider the following function-on-scalar regression problem. Let  $i = 1, \dots, N$  denote the  $N$  sampling units (e.g., subjects). Let  $t_{in}$ ,  $n = 1, \dots, N_i$ , denote the sampling times for subject  $i$  and define  $\mathbf{t}_i = (t_{i1}, \dots, t_{iN_i})$ ; we do not assume any structure on the  $\mathbf{t}_i$ 's across subjects. The observed response for subject  $i$  at time  $t_{in}$  is denoted  $y_{in} = y_i(t_{in}) \in \mathbb{R}$  and we define  $\mathbf{y}_i = y_i(\mathbf{t}_i) = (y_{i1}, \dots, y_{in_i}) \in \mathbb{R}^{n_i}$  as the vector of responses for subject  $i$ . In the present exposition, we assume the covariates  $\mathbf{x}_{in} = \mathbf{x}_i(t_{in}) \in \mathbb{R}^p$  to be constant through time, indicated by the absence of time index in  $\mathbf{x}_i \equiv \mathbf{x}_i(\cdot)$ , but our proposed model and implementation readily works for  $\mathbf{x}_{in} \in \mathbb{R}^p$  varying with time, provided it is observed at the same time points as the responses of subject  $i$ .

### 2.2 Varying Coefficient Mixed Model

Our main goal is to study the relationship between covariates  $\mathbf{x}_i$  and the functional response  $y_i(\cdot)$ , while accounting for temporal dependence within subjects and other covariates. In particular, we are interested in identifying *if, when* and *how*  $y_i(\cdot)$  changes with each entry in  $\mathbf{x}_i$ . To this end, we consider a *varying coefficient mixed model*:

$$\mathbb{E}\{y_{in} \mid \theta_i(t_{in})\} = \boldsymbol{\beta}(t_{in})^\top \mathbf{x}_i + \theta_i(t_{in}) \quad \text{Var}(y_{in} \mid \theta_i(t_{in})) = \sigma^2 \quad (1)$$

with (conditional) independence across  $i$  and  $n$ , where  $\boldsymbol{\beta}(\cdot) : \mathbb{R} \rightarrow \mathbb{R}^p$  is the vector-valued function of time-varying coefficients, and where  $\theta_i(\cdot)$  is a random process capturing the temporal dependence. In particular, we assume  $\mathbb{E}\{\theta_i(t)\} \equiv 0$  with covariance kernel  $\text{Cov}(\theta_i(t), \theta_i(t')) = \sigma^2 k_\theta(t, t')$  for some symmetric positive definite kernel  $k_\theta$ . Define  $\mathbf{K}_\theta(\mathbf{t})$  as the (unscaled) covariance matrix for a random process evaluated at the time points in  $\mathbf{t}$ , that is,  $[\mathbf{K}_\theta(\mathbf{t})]_{nn'} = k_\theta(t_n, t_{n'})$ . Hence, marginally, the response vector  $\mathbf{y}_i$  has mean  $\mathbf{m}_i := \boldsymbol{\beta}(\mathbf{t}_i)^\top \mathbf{x}_i$  and variance  $\mathbf{V}_i := \sigma^2 (\mathbf{K}_\theta(\mathbf{t}_i) + \mathbf{I}_{N_i})$ , where  $\boldsymbol{\beta}(\mathbf{t}_i)$  is the  $p \times N_i$  matrix with columns  $\boldsymbol{\beta}(t_{in})$ . Given  $S$  time points of interest  $\mathbf{t} = (t^{(1)}, \dots, t^{(S)})$ , we are interested in the value of  $\boldsymbol{\beta}(\cdot)$  at each of those

time points. For example,  $\mathbf{t}$  could consist of all observed time points or of a regular grid over the observed domain. We define  $\mathbf{B}$  as the  $p \times S$  matrix with entries  $b_j^{(s)} = \beta_j(t^{(s)})$ , with rows  $\mathbf{b}_j = \beta_j(\mathbf{t})$  and with columns  $\mathbf{b}^{(s)} = \beta(t^{(s)})$ .

To obtain the most efficient estimator of the mean parameters, we need  $\mathbf{V}_i$  to accurately capture the dependence structure in the residuals  $\mathbf{r}_i = \mathbf{y}_i - \mathbf{m}_i$ . For a regular design, i.e.,  $\mathbf{t}_i \equiv \mathbf{t}$  for some  $\mathbf{t}$ , and given  $N$  sufficiently large, we could simply estimate  $\mathbf{V} \equiv \mathbf{V}_i \approx \frac{1}{N} \sum_{i=1}^N \mathbf{r}_i \mathbf{r}_i^\top$ , perhaps with a prior smoothing step (Wang et al., 2022). For irregular designs, more care is required as empirical covariances are not applicable.

As observed by Fan et al. (2007), efficiency gains can be obtained even though the working covariance does not exactly match the true covariance. In particular, even a rough optimization of the working covariance can lead to near-optimal estimation efficiency. We propose to specify a working parametric model whose covariance function is determined by a few parameters. Some notable examples include the compound symmetry structure, equivalent to a random intercept model, with covariance function  $k_\theta(t, s; r_\theta) = r_\theta$ , and the AR(1) model, with covariance function  $k_\theta(t, s; r_\theta, \rho) = r_\theta \rho^{|t-s|}$ , where  $r_\theta$  denotes the variance ratio with the noise variance  $\sigma^2$  and where  $\rho$  controls the long-range dependency.

### 2.3 Local and Global Sparsity

A convenient feature of local regression is that the value of  $\beta(\cdot)$  at a specific time  $t^{(s)}$  is directly parameterized by  $\mathbf{b}^{(s)}$ . This is in contrast to spline basis expansions, where the value of  $\beta(t^{(s)})$  is a linear combination of basis functions active at time  $t^{(s)}$ . Hence, to find  $\beta_j(t^{(s)}) = 0$ , we only need  $b_j^{(s)} = 0$ , compared to requiring a consecutive set of spline weights to be zero. This allows us to use a simple sparsity-inducing penalty on the entries of  $\mathbf{B}$ , in comparison to overlapping group penalties used in spline methods (Wang and Kai, 2015; Tu et al., 2020; Wang et al., 2022; Zhong et al., 2022).

We thus propose to encourage local sparsity by including a Lasso penalty (Tibshirani,

1996) on  $\mathbf{B}$ , namely,  $\lambda \sum_{j=1}^p \sum_{s=1}^S \omega_j^{(s)} |b_j^{(s)}|$ , where  $\omega_j^{(s)}$  are weights and where  $\lambda \geq 0$  is the regularization parameter. While the Lasso penalty really only encourages *pointwise* sparsity, the combination of smoothing with this penalization encourages *local* sparsity, that is, sparsity across consecutive time points.

Furthermore, we may be interested in encouraging  $\beta_j(\cdot) \equiv 0$  altogether to identify if the  $j$ th covariate has any association with the response. This suggests to add a group lasso penalty on the whole vector  $\mathbf{b}_j$ , leading to the sparse group Lasso penalty (Friedman et al., 2010; Simon et al., 2013):

$$\mathcal{P}_{\lambda, \alpha}(\mathbf{B}; \Omega) := \lambda \sum_{j=1}^p \left[ (1 - \alpha) \sqrt{S} \omega_j \|\mathbf{b}_j\|_2 + \alpha \sum_{s=1}^S \omega_j^{(s)} |b_j^{(s)}| \right] \quad (2)$$

where  $\alpha \in [0, 1]$  is a tuning parameter balancing between encouraging global sparsity ( $\alpha = 0$ ) and local sparsity ( $\alpha = 1$ ), where  $\omega_j$  are weights for the group lasso penalty, and where  $\Omega$  contains all weights. We refer to Section S2.4 of the Supplementary Materials for experiments on the choice of  $\alpha$ .

The Lasso and group Lasso penalty are famously known for their estimation bias due to the shrinkage applied to non-zero values. To alleviate this issue, we propose to use adaptive penalties (Zou, 2006; Nardi and Rinaldo, 2008; Poignard, 2020), where the weights are set to  $\omega_j = \|\hat{\mathbf{b}}_j^{\text{mle}}\|_2^{-\gamma}$  and  $\omega_j^{(s)} = |\hat{b}_j^{(s), \text{mle}}|^{-\gamma}$  for some  $\gamma > 0$ , where  $\hat{\mathbf{B}}^{\text{mle}}$  contains the coefficients estimated without penalty.

## 2.4 Estimation

We alternate between mean parameter updates and variance parameter updates by holding the other fixed. We find that there is generally very little change beyond the first cycle and that a single variance update is often sufficient (similar to the two-step estimator of Wang et al., 2022).

*Kernel Smoothing.* Denote by  $\mathbf{X}_i$  the  $n_i \times p$  matrix with rows  $\mathbf{x}_{in}$ ; for fixed covariates, we simply have  $\mathbf{X}_i = \mathbf{1}_{n_i} \mathbf{x}_i^\top$ . We define the estimating function for  $\beta(t)$  by weighing the

residuals using a kernel function  $k_h(s) = k(s/h)/h$  depending on the distance from a time point of interest  $t$ , similarly to locally constant kernel smoothing (Wang et al., 2005):

$$U_{\beta(t)} := - \sum_{i=1}^N \mathbf{X}_i^\top \text{diag}(\mathbf{k}_i(t)) \mathbf{V}_i^{-1} \mathbf{r}_i, \quad (3)$$

where  $\mathbf{k}_i(t) = [k_h(t - t_{ij})]_{j=1}^{n_i}$ , where  $h > 0$  is the kernel scale. We employ kernel smoothing rather than spline smoothing as inducing zeros through penalization is simpler.

*Proximal Updates.* The penalized estimating functions are given by adding the subgradients of the penalty to the unpenalized functions, similarly to Wang et al. (2012) and Johnson et al. (2008) where a linear approximation to the penalty is rather used:

$$U_{\mathbf{b}_j} + \partial_{\mathbf{b}_j} P_{\lambda, \alpha}(\mathbf{B}; \Omega), \quad j = 1, \dots, p,$$

where  $U_{\mathbf{b}_j} = (U_{b_j^{(1)}}, \dots, U_{b_j^{(S)}}) \in \mathbb{R}^S$  is the estimating function for covariate  $j$ , and where  $\partial_{\mathbf{b}_j}$  denotes the subgradient with respect to  $\mathbf{b}_j$ .

Rather than considering a minorization-maximization scheme to solve the penalized estimating equation  $\mathbf{0} \in U_{\mathbf{b}_j} + \partial_{\mathbf{b}_j} P_{\lambda, \alpha}(\mathbf{B}; \Omega)$ , we utilize the convexity of the sparse group Lasso penalty to our advantage and proceed to proximal gradient updates. Specifically, we use the estimating function to perform a gradient step before applying the corresponding proximal operator (Parikh et al., 2014). We refer to Section S1.1 of the Supplementary Material for details on the proximal update.

*Covariance Parameters Estimation.* To estimate the variance parameters  $\boldsymbol{\tau}$ , we maximize the profile likelihood under a Gaussian model (equivalently, a quasi-likelihood approach, Fan and Wu, 2008) while holding the residuals  $\mathbf{r}_i$  fixed:

$$\ell(\boldsymbol{\tau}) := -\frac{1}{2} \sum_{i=1}^N \log \det(2\pi \mathbf{V}_i) + \mathbf{r}_i^\top \mathbf{V}_i^{-1} \mathbf{r}_i,$$

where  $\mathbf{V}_i$  implicitly depend on the variance parameters. Updates for the compound symmetry covariance can be found in Section S1.2 of the Supplementary Material.

## 2.5 Additional Details

We refer to the Supplementary Material for additional information and practical guidelines about LSVCM. In particular, we propose an *extended Bayesian information criterion* (EBIC, [Chen and Chen, 2008](#)) for selection of the regularization parameter  $\lambda$  and the kernel scale  $h$  (S1.3). Additionally, we utilize bootstrap sup-t simultaneous confidence bands ([Montiel Olea and Plagborg-Møller, 2019](#)) for uncertainty quantification (S1.4), which also enable the computation of  $p$ -values that can be used for multiplicity corrections (S1.5).

## 3. Simulation Studies

We consider two scenarios where the sampled time points  $\mathbf{t}_i$  vary between subjects. In the first case, subjects are sampled on a common set of time points  $\mathbf{t}$ , but not all time points are observed for each subject. This situation, inspired from our real data application in Section 4, occurs in experimental studies with missing data. In the second case, subjects are each sampled at different time points so that none or few time points are shared across subjects. This situation more commonly arises with observational studies, where researchers do not control sampling.

Synthetic data is generated as follows. We consider the task of estimating temporal group differences within  $N = 100$  subjects, half of which are assigned to either group. A random intercept  $\theta_i(t) \equiv \theta_i$  is sampled from a normal distribution centered at 0 with variance  $\sigma^2 r_\theta$ , where  $r_\theta$  denotes the variance ratio between noise and random effect. The mean function for each subject is computed as  $\mu_i(t) = \beta_0(t) + \beta_1(t)x_i$ , where  $x_i$  is the group indicator variable. Observations are finally generated as  $y_{ij} = \mu_i(t_{ij}) + \theta_i + \sigma\varepsilon$  for  $\varepsilon \sim \mathcal{N}(0, 1)$ . Unless specifically varied in an experiment, default values for variance parameters are  $\sigma^2 = 1$  and  $r_\theta = 1$ , leading to a correlation of 0.5 across time points. The true generating values for the

time-varying effects  $\beta_1(\cdot)$  will be defined in each sub-experiments such that it is smooth and non-zero only on part of the domain.

For both scenarios, we conduct four sub-experiments. In the first experiment, we vary the signal strength by increasing the variance  $\sigma^2$  while keeping the signal fixed. In the second experiment, we investigate the effect of missing data by varying the number of sampled time points per subject. In the third experiment, we study the effect of the dependence by varying the variance ratio parameter  $r_\theta$ . In the fourth experiment, we investigate the performance in relation to the sample size. We report the mean absolute estimation error (MAE) in estimating the functional group difference  $\beta_1(\cdot)$  as well as the classification accuracy induced by the sparsity, both of which over a pre-specified grid of time points. Additional performance metrics are included in Section S2.1 of the Supplementary Material.

Four methods are compared. Our proposed method, **LSVCMM**, is fitted with a compound symmetry variance structure, using a Gaussian kernel with a fixed kernel scale ( $h = 0.2$ ) and the regularization parameter is selected using the EBIC described in Section S1.3 of the Supplementary Materials. We also include **LSVCM**, which is the same as **LSVCMM**, except that an independent variance structure is used. **LSVCM** is closely related to the method of [Kong et al. \(2015\)](#) where a local linear approximation and a SCAD penalty is rather utilized. We further consider another simplification where the kernel smoothing is removed (**ALasso**): this amounts to independent sparse estimation at each time point, though estimation of  $\sigma^2$  and tuning parameter selection is done jointly. Finally, we include **SPFDA** ([Wang et al., 2022](#)) which is a direct competitor to **LSVCMM** as it includes smoothing, dependence and local sparsity, but it requires sampling times to be shared. To apply **SPFDA**, we impute the missing samples using functional PCA (fPCA, [Goldsmith et al., 2013](#)). The bridge penalty parameter is set to  $\alpha = 0.5$  and the regularization parameter is selected using their proposed EBIC.

### 3.1 Missing Data in Regular Design

In this scenario, we consider 10 time points regularly-spaced on the unit interval. To introduce missing data, we randomly select 71% of the time points and 71% of the subjects and set the intersection as missing, leading to, on average, 50% of the  $10 \times 100$  samples to be missing. With this procedure, only 29% of subjects will have 10 samples while the other 71% will only have around three. Symmetrically, three time points will be observed for all 100 subjects, while the remaining seven will only be observed for 29 subjects. The intercept function is chosen to be the zero function and the group difference function is set to be  $\sin(2\pi(t - \frac{1}{4})) \vee 0$  so that only the middle four time points are non-zero. SPFDA is fitted using 12 spline functions. Evaluation metrics, aggregated over the 10 time points, can be found in Figure 1.

[Figure 1 about here.]

Comparing LSVCMM to its independent counterpart, LSVCM, we find that the largest difference appears in the estimation error, especially for weak signal (large variance or large random effect). The cross-sectional method, **ALasso**, generally does worse in estimation and accuracy, except in very strong signal regimes, where it outperforms all others in accuracy. SPFDA performs similarly to LSVCMM in terms of estimation, apart from strong signal regimes, but does much worse in terms of support recovery. Additional metrics, featured in Figure S1 of the Supplementary Material show that SPFDA typically selects more time points as differential, leading to largely inflated FDR and slightly better power. In particular, as the proportion of missing data decreases, we would expect SPFDA to become comparable to LSVCMM, but accuracy actually decreases, interestingly.

### 3.2 Irregular Sampling

In this scenario, we mimic uniform sampling by using 100 regularly-spaced time points over the unit interval and uniformly draw 10 of those as observed for each subject. Then, each of the 100 time points is observed, on average, only 10 times. The intercept function is again

chosen to be the zero function and the group difference function as  $\text{sigmoid}(20(0.6 - t))\mathbb{1}[t < 0.45]$ , such that the first 45 time points are null. **SPFDA** is fitted using 50 splines. Evaluation metrics, aggregated over the 100 time points, can be found in Figure 2.

[Figure 2 about here.]

Cross-sectional methods have a much harder time with this setting since there are only a few observations at each time points: indeed, **ALasso** requires over 50 samples per time point before starting to estimate non-zero differences. In terms of dropping longitudinal effects (**LSVCM**), we observe the same pattern as in the missing data scenario, where weak signal and strong dependency produce worse performance. Additionally, we notice a much larger drop in accuracy as the sampling time become dense, where longitudinal effects are more noticeable. This setting is also more difficult for **SPFDA** as it will rely more heavily on the imputed observations: the transition from sparsely-observed data to densely-observed data makes this abundantly clear as the estimation error becomes comparable. Additionally, increasing the sample size widens the gap between **SPFDA** and **LSVCMM**, indicating that the imputation bias is a key component in explaining the difference in performance.

#### 4. Oral Cancer Development Mouse Study

The tumor suppressor gene *Dmbt1* (*deleted in malignant brain tumors 1*) plays a critical role in the progression of oral squamous cell carcinoma (SCC) (Singh et al., 2021). *Dmbt1* is present in human saliva, where it exhibits antimicrobial properties (Reichhardt et al., 2017). In a recent longitudinal study, Medeiros et al. (2023) found that *Dmbt1* levels varied with cancer progression and treatment and were associated with changes in microbial composition. To better understand the interaction between *Dmbt1*, microbial composition, and oral SCC development, a new mouse study was conducted (Medeiros et al, manuscript in preparation) were 76 mice were bred with (*wild type*, WT) and without (*knockout*, KO) the *Dmbt1* gene

before being inoculated with oral SCC. The saliva samples were then collected over time (0, 4, 8, 12, 16 and 22 weeks after inoculation) and 16S sequencing was performed (16S rRNA, 97% sequence similarity OTU binning). Finally, the histopathology of the tongue was evaluated at week 22 where the mice were diagnosed with pre-cancer *epithelial dysplasia* (ED) or *carcinoma in situ* (CIS), or with SCC. The results strengthen the original findings of [Singh et al. \(2021\)](#) as 17 of the 34 (50%) knockout mice and only 6 of the 42 (14%) wild type mice developed SCC by week 22, suggesting a *causal* link between Dmbt1 and cancer progression.

A potential avenue of action of Dmbt1 on cancer progression, as suggested by the findings in [Medeiros et al. \(2023\)](#), is through the microbiota. Therefore, one of the objectives of the study is to investigate the longitudinal association of microbial composition with the Dmbt1 genotype (WT vs. KO) and with diagnosis (dichotomized as precancer, ED / CIS, vs. cancer, SCC) . In particular, the identification of specific OTUs and weeks with differential abundance between any of the subgroups can reveal how Dmbt1 and the microbial composition influence cancer progression, potentially leading to better prediction of treatment response and individualized treatments. To this end, we consider the following VCM for the *centered log-ratio* (clr) transformed abundance of each OTU:

$$\begin{aligned} \mathbb{E}\{\text{clr}(y(w)) \mid \mathbf{x}\} = & \beta_0(w) + \beta_{\text{KO}}(w)x_{\text{KO}} + \beta_{\text{SCC}}(w)x_{\text{SCC}} \\ & + \beta_{\text{KO:SCC}}(w)x_{\text{KO}}x_{\text{SCC}} + \beta_{\text{F}}(w)x_{\text{F}}, \end{aligned} \quad (4)$$

where  $w$  denotes the week and where  $x_{\text{KO}}$ ,  $x_{\text{SCC}}$  and  $x_{\text{F}}$  are group indicators for genotype, diagnosis and sex, respectively.

An important challenge that emerges from data collection is a significant amount of missing data. Saliva samples were collected for only 65 mice and, of the  $6 \times 65 = 390$  potential samples, only 294 (75%) were ultimately sequenced. Figure 3 shows the number of samples available per week and per subgroup, along the missingness patterns.

[Figure 3 about here.]

We apply the LSVCMM methodology to VCM (4). After filtering out OTUs below 5% prevalence across the 294 samples, there remains 187 OTUs to be used as the response. We fit LSVCMM with a compound symmetry working covariance, with a Gaussian kernel, with a mixed penalty ( $\alpha = 0.5$ ) to encourage global sparsity in each of the terms as well as local sparsity to identify weeks of differential abundance. The intercept varying coefficient is not penalized since there is no expectation it should be close to 0. The regularization parameter  $\lambda$  and the kernel scale  $h$  is selected using the EBIC proposed in Section S1.3 of the Supplementary Material. We compare LSVCMM to **ALasso** (i.e., cross-sectional with sparsity), and to **SPFDA** (with fPCA imputation of the missing entires). We omit LSVCM from the comparison since, as was seen from the simulation studies in Section 3, the main difference is in estimation error, not selection accuracy. For LSVCMM and **ALasso**, we use bootstrap to obtain simultaneous confidence bands for all varying coefficients of interests. **SPFDA** only provides point-wise standard errors: we produce simultaneous bands using the provided standard error and a Bonferroni adjustment, corresponding to multiplying the standard error by a factor of 2.64, the upper  $1 - 0.025/6$  upper quantile of a standard normal distribution. For each of the two main effects of genotype and diagnosis and for their interaction terms, we report the estimated varying coefficients and note which weeks are such that zero was excluded. For brevity, only taxa identified as DA for at least one week by one method are reported, though 187 OTUs were processed.

[Figure 4 about here.]

Figure 4 contains the estimated varying coefficients for the main effects of genotype and diagnosis as well as for the interaction term. We generally find strong agreement between LSVCMM and its cross-sectional counter-part **ALasso** and some agreement between LSVCMM and **SPFDA**. **ALasso** tends to select more differences than LSVCMM, but many of the additional

discoveries occur for the weeks 4-16 where there are significantly more missing data. This is particularly obvious for the interaction term, where **ALasso** selects many OTUs at week 12. We note that **SPFDA** finds multiple small group differences among rare taxa (large OTU number) which are not corroborated by **LSVCMM** nor **ALasso**, suggesting that the standard error estimation may be inappropriate for those instances.

Five OTUs are identified by **LSVCMM** as having a non-zero interaction term, suggesting some interplay between the *Dmbt1* gene, the abundance of those OTUs and cancer development. In particular, OTU 0107 identifies a positive difference in the interaction term at week 0 and no differences in the main effects, suggesting that the KO mice with initially higher abundance of that OTU were more likely to develop SCC by week 22. Three OTUs, 0025, 0083 and 0318, have a negative interaction estimate at week 12. OTU 0025 does not have a non-zero main effect estimate, suggesting that KO mice with lower abundance of that OTU between week 12 and 16 were more likely to develop SCC by week 22. OTUs 0083 and 0318 also show a positive difference between diagnosis, indicating that WT mice with higher abundance of those two OTUs at week 12 were more likely to be diagnosed with SCC by week 22. Finally, OTU 0054 has a positive interaction estimate at week 16 and no non-zero main effect estimates, suggesting that KO mice with higher abundance of that OTU at week 16 were more likely to be diagnosed with SCC. All identified OTUs belong to taxonomic families known to be associated with oral SCC (Ahn et al., 2012; Olsen and Yilmaz, 2019) or with other digestive tract cancers (Flemer et al., 2018; Dong et al., 2019; Yoon et al., 2021).

## 5. Discussion

**LSVCMM** addresses two main deficiencies in existing sparse VCM methodologies. First, it includes longitudinal effects in the form of a parametric working covariance model, whereas many methods cannot account for within-subject dependencies (Wang and Kai, 2015; Kong et al., 2015; Tu et al., 2020; Zhong et al., 2022). Simulation experiments in Section 3 have

shown that omitting the dependency leads to worse estimation accuracy and worse support recovery in the densely sampled regime. Second, our proposed approach applies to any sampling design: in particular, it allows missing data in regular designs as well as irregular designs, where the only method including longitudinal effects (Wang et al., 2022, SPFDA) is limited to regular designs. Experiments show that imputation is insufficient in extending SPFDA to irregular cases, as support recovery is inferior to LSVCMM.

There are multiple avenues of improvement, not only in terms of general enhancements, but also with respect to the longitudinal differential abundance application of Section 4. First, the bootstrap simultaneous confidence bands are expensive to compute: indeed, in order to have a granular enough estimate of the quantiles, thousands of samples are required. A natural alternative would be to consider ideas from the *de-biased Lasso* literature (Zhang and Zhang, 2014; Honda, 2021). Second, while computationally convenient, the working covariance model requires some assumption on the dependency structure which could lead to misspecification. In Section S2.2 of the Supplementary Materials, we consider an experiment where the working covariance is misspecified and found that LSVCMM still improves on the independent model and on SPFDA. That being said, more severe misspecification could be troublesome and an alternative treatment of the dependency might be more robust. Third, the locally-constant kernel smoothing was similarly chosen for the ease of calculation, but it introduces some bias at the boundary of the domain and in regions of sharp variations: another important extension involves higher-order approximations such as the commonly-used local linear approximation. Fourth, utilizing a least square objective for the log-transformed microbial abundances is generally inappropriate, largely due to the zero-inflation occurring for rarer taxa. For example, 78 of the 187 OTUs considered have more than 90% of zeros across the 265 samples and 173 have more than 50% of zeros. A natural extension of LSVCMM would be to allow more general distribution, similarly to GLMs; in particular, a

negative binomial or Tweedie compound Poisson-Gamma objective would be of interest for our application. Of note, Zhong et al. (2022) is defined for *generalized* VCM, though it lacks longitudinal effects. Fifth, we processed each OTU independently, and there are two important sources of dependency among them that are thus disregarded. The sequencing procedure introduces negative dependence between OTUs because of compositionality effects, and OTUs corresponding to related species may have positive dependency which could be captured by the taxonomic tree. Both of these suggest a multivariate extension.

#### ACKNOWLEDGEMENTS

Nisha J D'Silva's research was supported by the National Institutes of Health grant R35DE027551. Gen Li's research was partially supported by the National Institutes of Health grant R03DE031296. This research was supported in part through computational resources and services provided by Advanced Research Computing at the University of Michigan, Ann Arbor. Computations for this research were also performed in part on the Pennsylvania State University's Institute for Computational and Data Sciences' Roar Collab supercomputer.

#### SUPPLEMENTARY MATERIALS

Appendix: Additional details on estimation (S1.1 and S1.2), tuning parameter selection (S1.3), simultaneous confidence bands (S1.4) and significance (S1.5), additional simulations results (S2.1), and misspecification experiments (S2.2). (PDF file)

R package for LSVCMM: R-package **LSVCMM** implementing the proposed methodology. (GNU zipped tar file; see also the GitHub repository [github.com/fontaine618/LSVCMM](https://github.com/fontaine618/LSVCMM), version 0.0.5)

R scripts: Code for running the experiments and producing the results included in the text. (GNU zipped tar file; see also the GitHub repository [github.com/fontaine618/LSVCMM-Experiments](https://github.com/fontaine618/LSVCMM-Experiments))

## DATA AVAILABILITY

The data underlying this article will be shared on reasonable request to the corresponding author.

## REFERENCES

Ahn, J., Segers, S., and Hayes, R. B. (2012). Periodontal disease, *Porphyromonas gingivalis* serum antibody levels and orodigestive cancer mortality. *Carcinogenesis* **33**, 1055–1058.

Chen, J. and Chen, Z. (2008). Extended Bayesian information criteria for model selection with large model spaces. *Biometrika* **95**, 759–771.

Daye, Z. J., Xie, J., and Li, H. (2012). A Sparse Structured Shrinkage Estimator for Nonparametric Varying-Coefficient Model With an Application in Genomics. *Journal of Computational and Graphical Statistics* **21**, 110–133.

Dong, Z., Chen, B., Pan, H., Wang, D., Liu, M., Yang, Y., Zou, M., Yang, J., Xiao, K., Zhao, R., Zheng, X., Zhang, L., and Zhang, Y. (2019). Detection of Microbial 16S rRNA Gene in the Serum of Patients With Gastric Cancer. *Frontiers in Oncology* **9**,.

Fan, J., Huang, T., and Li, R. (2007). Analysis of Longitudinal Data With Semiparametric Estimation of Covariance Function. *Journal of the American Statistical Association* **102**, 632–641.

Fan, J. and Wu, Y. (2008). Semiparametric Estimation of Covariance Matrixes for Longitudinal Data. *Journal of the American Statistical Association* **103**, 1520–1533.

Flemer, B., Warren, R. D., Barrett, M. P., Cisek, K., Das, A., Jeffery, I. B., Hurley, E., O’Riordain, M., Shanahan, F., and O’Toole, P. W. (2018). The oral microbiota in colorectal cancer is distinctive and predictive. *Gut* **67**, 1454–1463.

Friedman, J., Hastie, T., and Tibshirani, R. (2010). A note on the group lasso and a sparse group lasso. arXiv:1001.0736 [math, stat].

Goldsmith, J., Greven, S., and Crainiceanu, C. (2013). Corrected Confidence Bands for Functional Data Using Principal Components. *Biometrics* **69**, 41–51.

Gomaa, E. Z. (2020). Human gut microbiota/microbiome in health and diseases: a review. *Antonie van Leeuwenhoek* **113**, 2019–2040.

Gu, C. (2013). *Smoothing Spline ANOVA Models*, volume 297 of *Springer Series in Statistics*. Springer, New York, NY.

Honda, T. (2021). The de-biased group Lasso estimation for varying coefficient models. *Annals of the Institute of Statistical Mathematics* **73**, 3–29.

Johnson, B. A., Lin, D. Y., and Zeng, D. (2008). Penalized Estimating Functions and Variable Selection in Semiparametric Regression Models. *Journal of the American Statistical Association* **103**, 672–680.

Kong, D., Bondell, H. D., and Wu, Y. (2015). Domain selection for the varying coefficient model via local polynomial regression. *Computational Statistics & Data Analysis* **83**, 236–250.

Lee, E. R. and Mammen, E. (2016). Local linear smoothing for sparse high dimensional varying coefficient models. *Electronic Journal of Statistics* **10**, 855–894.

Lin, Z., Cao, J., Wang, L., and Wang, H. (2017). Locally Sparse Estimator for Functional Linear Regression Models. *Journal of Computational and Graphical Statistics* **26**, 306–318.

Luo, D., Ziebell, S., and An, L. (2017). An informative approach on differential abundance analysis for time-course metagenomic sequencing data. *Bioinformatics* **33**, 1286–1292.

Medeiros, M. C. d., The, S., Bellile, E., Russo, N., Schmitd, L., Danella, E., Singh, P., Banerjee, R., Bassis, C., Murphy, G. R., Sartor, M. A., Lombaert, I., Schmidt, T. M., Eisbruch, A., Murdoch-Kinch, C. A., Rozek, L., Wolf, G. T., Li, G., Chen, G. Y., and D’Silva, N. J. (2023). Salivary microbiome changes distinguish response

to chemoradiotherapy in patients with oral cancer. *Microbiome* **11**, 1–23.

Metwally, A. A., Yang, J., Ascoli, C., Dai, Y., Finn, P. W., and Perkins, D. L. (2018). MetaLonDA: a flexible R package for identifying time intervals of differentially abundant features in metagenomic longitudinal studies. *Microbiome* **6**, 32.

Metwally, A. A., Zhang, T., Wu, S., Kellogg, R., Zhou, W., Contrepois, K., Tang, H., and Snyder, M. (2022). Robust identification of temporal biomarkers in longitudinal omics studies. *Bioinformatics* **38**, 3802–3811.

Montiel Olea, J. L. and Plagborg-Møller, M. (2019). Simultaneous confidence bands: Theory, implementation, and an application to SVARs. *Journal of Applied Econometrics* **34**, 1–17.

Nardi, Y. and Rinaldo, A. (2008). On the asymptotic properties of the group lasso estimator for linear models. *Electronic Journal of Statistics* **2**, 605–633.

Noh, H. S. and Park, B. U. (2010). Sparse Varying Coefficient Models for Longitudinal Data. *Statistica Sinica* **20**, 1183–1202.

Ogunrinola, G. A., Oyewale, J. O., Oshamika, O. O., and Olasehinde, G. I. (2020). The Human Microbiome and Its Impacts on Health. *International Journal of Microbiology* **2020**, e8045646.

Olsen, I. and Yilmaz, O. (2019). Possible role of *Porphyromonas gingivalis* in orodigestive cancers. *Journal of Oral Microbiology* **11**, 1563410.

Parikh, N., Boyd, S., and others (2014). Proximal algorithms. *Foundations and trends® in Optimization* **1**, 127–239. Publisher: Now Publishers, Inc.

Paulson, J. N., Talukder, H., and Bravo, H. C. (2017). Longitudinal differential abundance analysis of microbial marker-gene surveys using smoothing splines.

Poignard, B. (2020). Asymptotic theory of the adaptive Sparse Group Lasso. *Annals of the Institute of Statistical Mathematics* **72**, 297–328.

Reichhardt, M. P., Holmskov, U., and Meri, S. (2017). SALSA-A dance on a slippery floor with changing partners. *Molecular Immunology* **89**, 100–110.

Shields-Cutler, R. R., Al-Ghalith, G. A., Yassour, M., and Knights, D. (2018). SplinecurveR Enables Group Comparisons in Longitudinal Microbiome Studies. *Frontiers in Microbiology* **9**,

Simon, N., Friedman, J., Hastie, T., and Tibshirani, R. (2013). A Sparse-Group Lasso. *Journal of Computational and Graphical Statistics* **22**, 231–245.

Singh, P., Banerjee, R., Piao, S., Costa de Medeiros, M., Bellile, E., Liu, M., Damodaran Puthiya Veettill, D., Schmitd, L. B., Russo, N., Danella, E., Inglehart, R. C., Pineault, K. M., Wellik, D. M., Wolf, G., and D'Silva, N. J. (2021). Squamous cell carcinoma subverts adjacent histologically normal epithelium to promote lateral invasion. *The Journal of Experimental Medicine* **218**, e20200944.

Staicu, A.-M., Lahiri, S. N., and Carroll, R. J. (2015). Significance tests for functional data with complex dependence structure. *Journal of Statistical Planning and Inference* **156**, 1–13.

Tibshirani, R. (1996). Regression Shrinkage and Selection Via the Lasso. *Journal of the Royal Statistical Society: Series B (Methodological)* **58**, 267–288.

Tu, C. Y., Park, J., and Wang, H. (2020). Estimation of Functional Sparsity in Nonparametric Varying Coefficient Models for Longitudinal Data Analysis. *Statistica Sinica* **30**, 439–465.

Wang, H. and Kai, B. (2015). Functional Sparsity: Global Versus Local. *Statistica Sinica* **25**, 1337–1354.

Wang, H. and Xia, Y. (2009). Shrinkage Estimation of the Varying Coefficient Model. *Journal of the American Statistical Association* **104**, 747–757.

Wang, L., Li, H., and Huang, J. Z. (2008). Variable Selection in Nonparametric Varying-

Coefficient Models for Analysis of Repeated Measurements. *Journal of the American Statistical Association* **103**, 1556–1569.

Wang, L., Zhou, J., and Qu, A. (2012). Penalized Generalized Estimating Equations for High-Dimensional Longitudinal Data Analysis. *Biometrics* **68**, 353–360.

Wang, N., Carroll, R. J., and Lin, X. (2005). Efficient Semiparametric Marginal Estimation for Longitudinal/Clustered Data. *Journal of the American Statistical Association* **100**, 147–157.

Wang, Z., Magnotti, J., Beauchamp, M. S., and Li, M. (2022). Functional group bridge for simultaneous regression and support estimation. *Biometrics* .

Xue, L. and Qu, A. (2012). Variable selection in high-dimensional varying-coefficient models with global optimality. *The Journal of Machine Learning Research* **13**, 1973–1998.

Yoon, Y., Kim, G., Jeon, B.-N., Fang, S., and Park, H. (2021). Bifidobacterium Strain-Specific Enhances the Efficacy of Cancer Therapeutics in Tumor-Bearing Mice. *Cancers* **13**, 957.

Zhang, C.-H. and Zhang, S. S. (2014). Confidence Intervals for Low Dimensional Parameters in High Dimensional Linear Models. *Journal of the Royal Statistical Society Series B: Statistical Methodology* **76**, 217–242.

Zhong, R., Zhang, C., and Zhang, J. (2022). Locally sparse estimator of generalized varying coefficient model for asynchronous longitudinal data. arXiv:2206.04315 [stat].

Zou, H. (2006). The Adaptive Lasso and Its Oracle Properties. *Journal of the American Statistical Association* **101**, 1418–1429.

Received August 2024. Revised May 2025. Accepted August 2025.

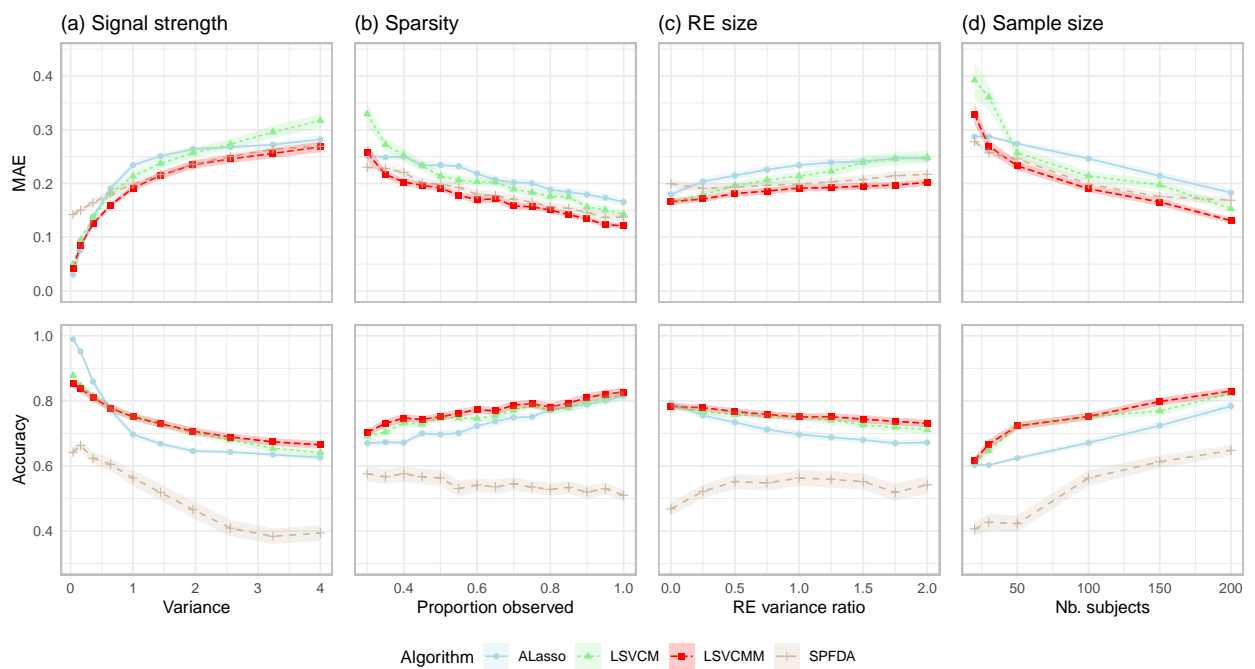


**Figure 1.** Evaluation metrics in the missing data scenario reported as the mean (line) and standard error (band) across 100 replications.

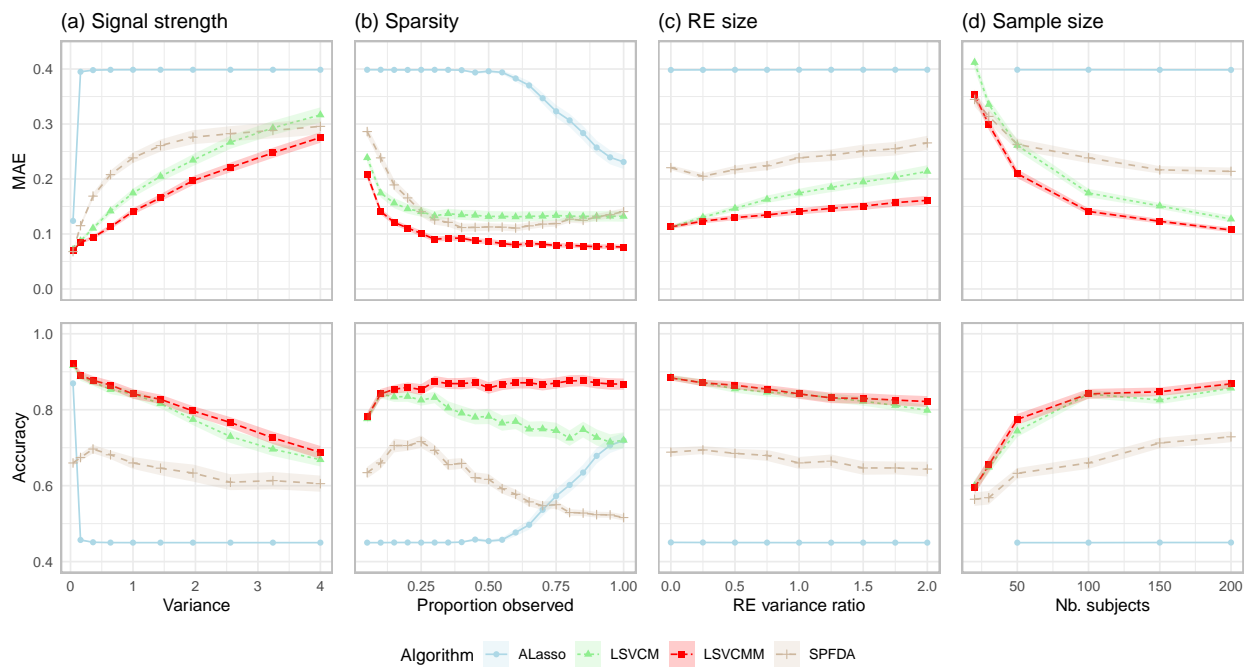


**Figure 2.** Evaluation metrics in the irregular sampling scenario reported as the mean (line) and standard error (band) across 100 replications.

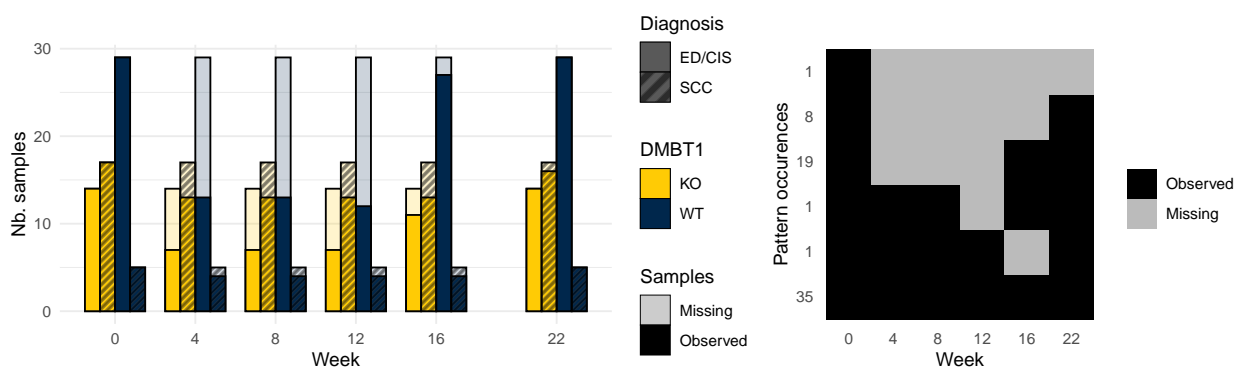


**Figure 3.** (Left) Number of observed and missing samples per week, stratified by genotype and diagnosis. (Right) Patterns of missingness; row labels indicate the frequency of that pattern occurring among the 65 mice.

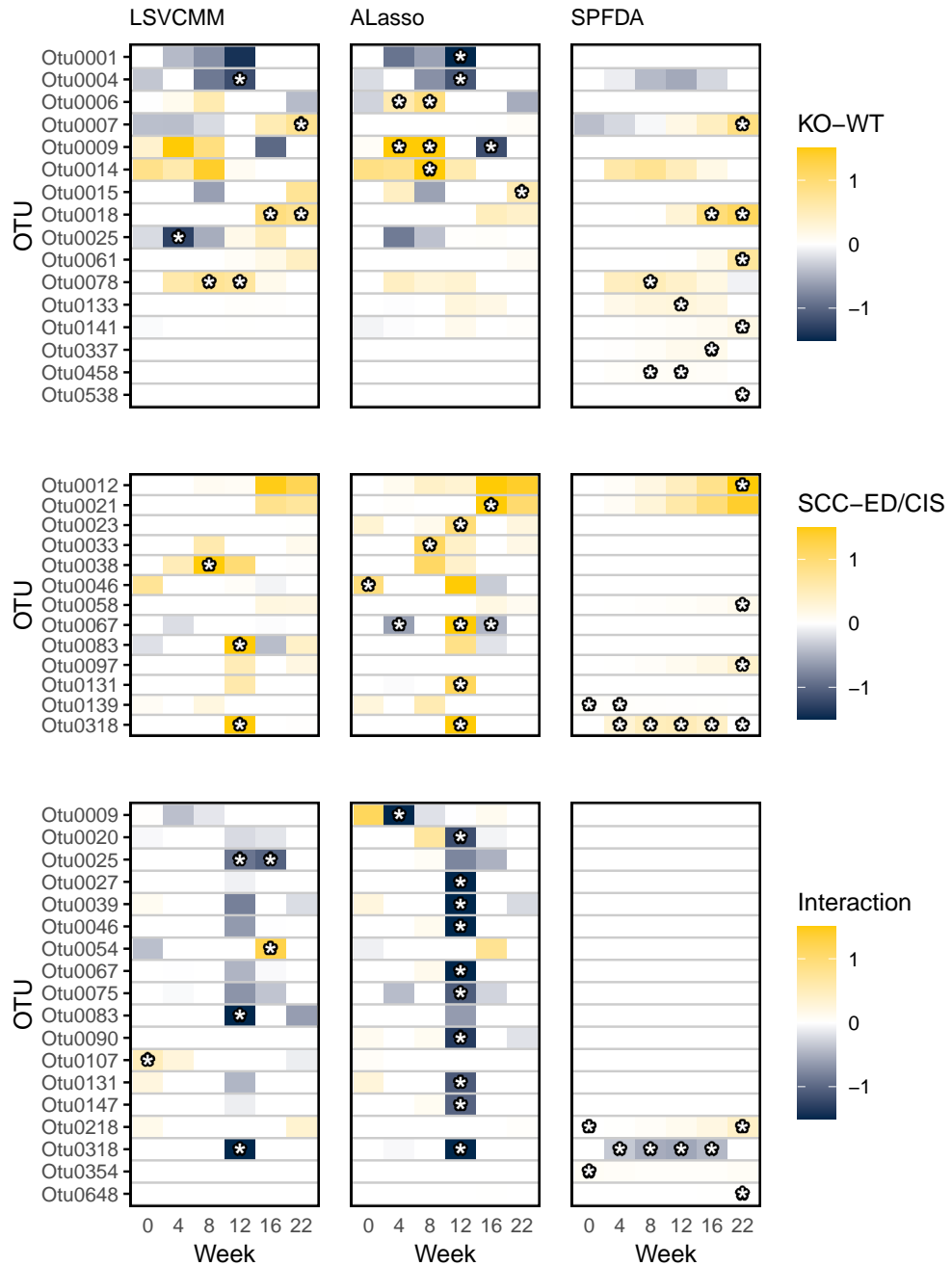


**Figure 4.** Estimated main effects (top: KO less WT; middle: SCC less ED/CIS) and interaction (bottom: coded as 1 if KO and SCC, and 0 otherwise). White cells correspond to a zero estimate, colored cells correspond to a non-zero estimate. Asterisks indicate a time point where the 95% simultaneous confidence band excludes zero. Columns represent estimate emerging from three different methods. Only OTUs with a significant difference for at least one time point and one method are included in each row (out of 187 total OTUs).